Tunable polymer lens

G. Beadie[1*], M. L. Sandrock[1], M. J. Wiggins[1], R. S. Lepkowicz[1†], and J. S. Shirk[1]
M. Ponting[2], Y. Yang [2], T. Kazmierczak[2], A. Hiltner[2], and E. Baer[2]

[1]Division of Optical Sciences, U. S. Naval Research Laboratory, Washington, DC 20375
[2]Department of Macromolecular Science and Engineering, Center for Applied Polymer Research, Case Western Reserve University, Cleveland, OH 44106, USA
[†]Now at Dept. of Physics and Optical Engineering, Rose-Hulman Institute of Technology, Terre Haute, IN 47803
**Corresponding author: guy.beadie@nrl.navy.mil*

Abstract: A new type of solid-state variable focal length lens is described. It is based on shape changes in an elastomeric membrane driven by compression of a reservoir of a polymer gel. A novel fabrication process based on individual lens components allows for customization of lens power based on the desired application. The lens shape as a function of applied compressive strain is measured using direct surface profile measurements. The focal length of a solid state lens was reversibly changed by a factor of 1.9. Calculated back focal lengths of the lens were consistent with experimental measurements.

©2008 Optical Society of America

OCIS codes: (110.1080) Adaptive optics; (220.3630) Lenses; (160.5470) Polymers

References and links

1. M. F. Land, and D.-E. Nilsson, *Animal Eyes* (Oxford University Press, Oxford; New York, 2002).
2. H. W. Ren, Y. H. Fan, S. Gauza, and S. T. Wu, "Tunable-focus flat liquid crystal spherical lens," Appl. Phys. Lett. **84**, 4789-4791 (2004).
3. H. W. Ren, D. W. Fox, B. Wu, and S. T. Wu, "Liquid crystal lens with large focal length tunability and low operating voltage," Opt. Express **15**, 11328-11335 (2007).
4. P. J. Smith, C. M. Taylor, E. M. McCabe, D. R. Selviah, S. E. Day, and L. G. Commander, "Switchable fiber coupling using variable-focal-length microlenses," Rev. Sci. Instrum. **72**, 3132-3134 (2001).
5. A. Raighne, T. Scharf, and E. M. McCabe, "Emerging light fields from liquid crystal microlenses," Rev. Sci. Instrum. **77**, 055103 (2006).
6. K. H. Jeong, G. L. Liu, N. Chronis, and L. P. Lee, "Tunable microdoublet lens array," Opt. Express **12**, 2494-2500 (2004).
7. D. Y. Zhang, N. Justis, and Y. H. Lo, "Fluidic adaptive zoom lens with high zoom ratio and widely tunable field of view," Opt Commun **249**, 175-182 (2005).
8. D. Y. Zhang, V. Lien, Y. Berdichevsky, J. Choi, and Y. H. Lo, "Fluidic adaptive lens with high focal length tunability," Appl. Phys. Lett. **82**, 3171-3172 (2003).
9. S. W. Lee, and S. S. Lee, "Focal tunable liquid lens integrated with an electromagnetic actuator," Appl. Phys. Lett. **90**, 121129 (2007).
10. H. W. Ren, D. Fox, P. A. Anderson, B. Wu, and S. T. Wu, "Tunable-focus liquid lens controlled using a servo motor," Opt. Express **14**, 8031-8036 (2006).
11. H. W. Ren, and S. T. Wu, "Variable-focus liquid lens," Opt. Express **15**, 5931-5936 (2007).
12. P. M. Moran, S. Dharmatilleke, A. H. Khaw, K. W. Tan, M. L. Chan, and I. Rodriguez, "Fluidic lenses with variable focal length," Appl. Phys. Lett. **88**, 041120 (2006).
13. B. Berge, and J. Peseux, "Variable focal lens controlled by an external voltage: An application of electrowetting," Eur. Phys. J. E **3**, 159-163 (2000).
14. B. H. W. Hendriks, S. Kuiper, M. A. J. Van As, C. A. Renders, and T. W. Tukker, "Electrowetting-based variable-focus lens for miniature systems," Opt. Rev. **12**, 255-259 (2005).
15. T. Krupenkin, S. Yang, and P. Mach, "Tunable liquid microlens," Appl. Phys. Lett. **82**, 316-318 (2003).
16. S. Kuiper, and B. H. W. Hendriks, "Variable-focus liquid lens for miniature cameras," Appl. Phys. Lett. **85**, 1128-1130 (2004).
17. A. L. Glebov, L. D. Huang, S. Aoki, M. Lee, and K. Yokouchi, "Planar hybrid polymer-silica microlenses with tunable beamwidth and focal length," IEEE Photonics Tech. Lett. **16**, 1107-1109 (2004).
18. S. N. Lee, H. W. Tung, W. C. Chen, and W. L. Fang, "Thermal actuated solid tunable lens," IEEE Photonics Tech. Lett. **18**, 2191-2193 (2006).
19. M. Bass, *Optical Society of America Handbook of Optics, Volume II, Devices, measurements, and properties* (McGraw-Hill, New York, 1995).

#96331 - $15.00 USD Received 16 May 2008; revised 17 Jul 2008; accepted 17 Jul 2008; published 24 Jul 2008
(C) 2008 OSA

Report Documentation Page

Form Approved
OMB No. 0704-0188

Public reporting burden for the collection of information is estimated to average 1 hour per response, including the time for reviewing instructions, searching existing data sources, gathering and maintaining the data needed, and completing and reviewing the collection of information. Send comments regarding this burden estimate or any other aspect of this collection of information, including suggestions for reducing this burden, to Washington Headquarters Services, Directorate for Information Operations and Reports, 1215 Jefferson Davis Highway, Suite 1204, Arlington VA 22202-4302. Respondents should be aware that notwithstanding any other provision of law, no person shall be subject to a penalty for failing to comply with a collection of information if it does not display a currently valid OMB control number.

1. REPORT DATE	2. REPORT TYPE	3. DATES COVERED
17 JUL 2008		**00-00-2008 to 00-00-2008**

4. TITLE AND SUBTITLE	5a. CONTRACT NUMBER
Tunable polymer lens	5b. GRANT NUMBER
	5c. PROGRAM ELEMENT NUMBER
6. AUTHOR(S)	5d. PROJECT NUMBER
	5e. TASK NUMBER
	5f. WORK UNIT NUMBER
7. PERFORMING ORGANIZATION NAME(S) AND ADDRESS(ES) **Case Western Reserve University,Cleveland,OH,44106**	8. PERFORMING ORGANIZATION REPORT NUMBER
9. SPONSORING/MONITORING AGENCY NAME(S) AND ADDRESS(ES)	10. SPONSOR/MONITOR'S ACRONYM(S)
	11. SPONSOR/MONITOR'S REPORT NUMBER(S)

12. DISTRIBUTION/AVAILABILITY STATEMENT
Approved for public release; distribution unlimited

13. SUPPLEMENTARY NOTES

14. ABSTRACT
see report

15. SUBJECT TERMS

16. SECURITY CLASSIFICATION OF:			17. LIMITATION OF ABSTRACT	18. NUMBER OF PAGES	19a. NAME OF RESPONSIBLE PERSON
a. REPORT **unclassified**	b. ABSTRACT **unclassified**	c. THIS PAGE **unclassified**	**Same as Report (SAR)**	**11**	

20. M. J. Wiggins, J. M. Anderson, and A. Hiltner, "Biodegradation of polyurethane under fatigue loading," J. Biomed. Mater. Res. A **65**, 524-535 (2003).

1. Introduction

Today's technology is driving the need for lighter, simpler, and more compact optical devices, yet the requirements for image quality are only getting more stringent. Zoom capability, for example, is still desirable in even the smallest devices. Typical zoom lens systems need lens groups to move back and forth to adjust the image size. At a certain package size, one simply runs out of room to move lenses enough to magnify an image. Even for larger cameras, an alternative to mechanical motion would be beneficial by reducing engineering complexity. A fundamental shift in the design of zoom systems can occur if one considers variable lenses: mutable lenses which alter their shape or index distribution to produce focal length changes, without translational movement. This paper describes the fabrication and optical performance of an all-solid-state variable focal length lens developed to address these needs.

One need not look far for an example of a variable lens: the human eye changes its shape and refractive index in order to achieve dynamic focus [1]. Several research groups have embarked on biomimetic research projects in order to emulate the processes of the human eye. There has been work using voltage-controlled liquid crystals as active optical elements, for standard imaging systems as well as for fiber coupling [2-5]. Other variable lenses have been based on shape changes. Microfluidics enables the controlled injection of fluid into chambers with deformable membranes [6-8]. Fluid re-distribution can also be initiated mechanically to produce variable lenses [9-11]. Recent work shows lens properties of a controlled liquid drop shape, with no membrane [12]. A similar shape change based on different physics is found by taking advantage of electrowetting, in which an electrically induced change in surface-tension changes the surface curvature of liquid microlenses [13-16].

In contrast to the liquid tunable lenses, an all-solid-state polymer lens more closely mimics the nature of the human eye lens. Solid-state lenses can more readily withstand fluctuations in temperature, pressure, and motion than liquid based lenses and offer a more robust approach to tunable optical systems. To our knowledge, very little research has been published in this arena. Thermopolymers have been used recently to create a tunable microlens and lens array [17, 18]. In that device, adjusting the temperature of the thermo-optical polymer within the lens can change the focal properties.

This work discusses the development and characterization of an all-polymer tunable lens, in which pressure applied to a membrane containing a compliant cross-linked polymer gel causes symmetric shape changes to the outer surface. A detailed description of lens fabrication, detailing the materials used in the construction, their properties, and how they are assembled into the lenses is presented. An analysis of lens shape change, including direct measurements of the surface profiles as a function of applied pressure, is discussed. The focal length is measured as a function of applied stress and correlated with the tunable surface shape as a model to predict lens focal length change.

#96331 - $15.00 USD Received 16 May 2008; revised 17 Jul 2008; accepted 17 Jul 2008; published 24 Jul 2008
(C) 2008 OSA

2. Results

2.1 Fabrication

A novel lens manufacturing procedure was developed to fabricate solid state deformable composite lenses. Composite, variable focal length lens designs were created through the production of individual optical components: a flexible, elastomeric lens membrane, a reservoir of cross-linked gel-like polymer beneath the membrane, hard plastic backings, and static hard plastic lenses. Fabrication of lenses through assembly of the individual components provided an advantage in their flexibility to be aligned and integrated in several different geometries to form a lens of tailored static and variable optical power. A general description following the fabrication of the optical components and composite lens is shown in Fig. 1.

Composite, variable focal length lenses were constructed using a combination of deformable and rigid polymeric materials. An elastomeric styrene-ethylene/butylene-styrene (SEBS) block copolymer was provided by Kraton Polymers (Kraton® G1657). A room temperature, cross-linkable, two-part polydimethyl siloxane (PDMS) was provided by Dow Corning Corp. (Sylgard® 184). Poly (methyl methacrylate) (PMMA) was provided by Atofina Chemicals, Inc. (Plexiglas V920). The SEBS copolymer and PMMA resins were received in pellet form and used without further modification. The cross-linkable PDMS was received as a viscous fluid and cross-linked at a w/w ratio of 40:1.

The deformable elastomers and rigid PMMA materials were selected based on material optical properties (refractive index, transmission, and high clarity). The refractive indices of the Kraton and PDMS were measured at three wavelengths, Table 1, using a commercial instrument (Model 2010 Prism Coupler, Metricon Corporation, Pennington, NJ). Also reported are the indices interpolated from standard data on PMMA [19]. In addition to optical requirements, elastomers were selected based on an ability to reversibly change shape with pressure. Reversible expansion of the elastomeric membrane was ensured through application of tuning strains less than the elastic deformation limit of the SEBS rubber. It is estimated that the maximum strain on the lenses in this paper was 18%, as compared to the irreversible strain limit which lies between 30% and 40%.

Table 1. Materials used in the fabrication of tunable lenses.

Material	Trade Name	Lens Component	Refractive Indices		
			532 nm	633 nm	1544 nm
SEBS Rubber	Kraton G1657	Deformable membrane & spacer	1.4938	1.4886	1.4785
PDMS Elastomer	Slygard 184	Elastomer core	1.4149	1.4107	1.4002
PMMA	Plexiglas V-920	Static lens	1.4955	1.4908	1.4794

Soft, deformable meniscus shaped lens membranes were created via compression molding of SEBS elastomer, Fig. 1(a). A sheet of SEBS was placed between a plano-convex and plano-concave glass lens which were housed and aligned in a metal holder. An additional metal spacer of designated height was placed around the lens holders to regulate the thickness of the deformable lens shell. The assembly was molded at 120^{o}C for 15 minutes under slight pressure, cooled in-situ, and removed from the holder assembly.

Rigid lenses of desired geometry were fabricated via compression molding of PMMA sheet utilizing the commercial glass lens and lens holder design previously described to manufacture deformable SEBS lens membranes. The flexibility of this manufacturing

#96331 - $15.00 USD Received 16 May 2008; revised 17 Jul 2008; accepted 17 Jul 2008; published 24 Jul 2008
(C) 2008 OSA

method allowed for variation in the glass shape and geometry to produce PMMA lenses of corresponding shape and geometry. In this study, plano-convex and plano-concave PMMA lenses of various radii of curvature were fabricated via this method for inclusion in the composite, variable focal length lenses.

The PMMA lenses were aligned and attached to an optically smooth, flat molded PMMA backing for ease of incorporation into the final composite lens design. An ultra violet cross-linking optical adhesive (Dymax OP-29V, Dymanx Corp., Torrington CT) was applied between the lens and flat backing. Upon exposure to UV light, the lens and backing assembly were irreversibly attached.

Soft, SEBS elastomer spacers were created via compression molding of virgin resin pellets at 190°C under 10,000 lb_f for 5 minutes, Fig. 1(a). A metal spacer was utilized to assure a final sheet thickness of 4 mm. Circular spacers were cut from the flexible sheet using custom machined die punches of designated diameter. A second mechanical punching of the circular spacer resulted in the creation of soft rings using a second die punch of smaller diameter. 25 and 20 mm diameter circular die punches were utilized to create ring-like, soft, SEBS spacers for the variable focal length lens designs described in this work.

Composite, variable focal length lenses were created through the alignment and adhesion of the previously described optical components. As shown in Fig. 1(b), the multi-step assembly procedure began with the adhesion of the SEBS spacer onto the SEBS deformable meniscus lens membrane. Adhesion was completed via a two-part bonder/activator cyanoacrylate glue (Loctite®, Henkel Corporation, Avon, OH). An additional adhesion of the rigid PMMA lens and backing followed.

PDMS monomer was mixed with a cross-linking agent at a w/w ratio of 40:1. The elastomer was injected, via syringe, through the SEBS spacer and into the air filled cavity of the composite lens, Fig. 1(c). A second syringe was inserted through the SEBS spacer to allow for the displaced air to vent from the lens cavity during injection. The elastomer filled composite lens was allowed to cross-link at room temperature for three days before optical testing and analysis were performed.

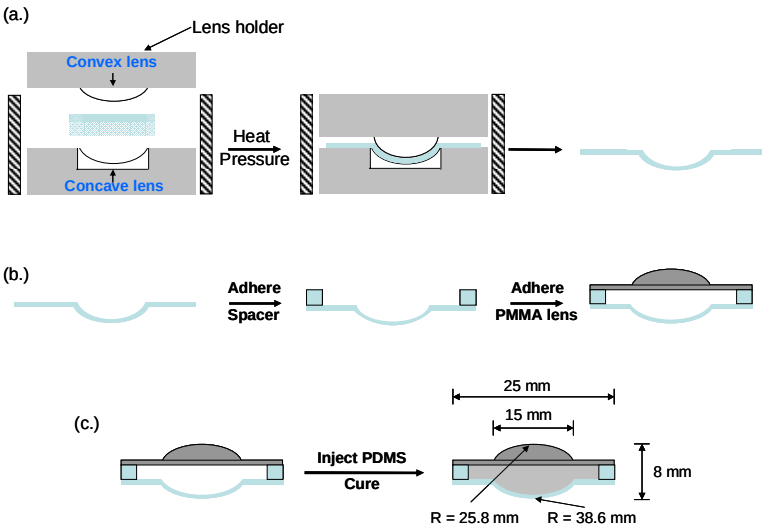

Fig. 1. Fabrication and assembly of variable focal length lens. (a). Fabrication of deformable membrane, (b). Assembly of variable focal length lens, (c). Final injection and cure of PDMS lens core. Final diagram labeled with dimensions of lens tested in this work.

Concave-convex, double convex, and plano-convex lens designs have been successfully fabricated using the methods outlined in Fig. 1. In this paper the mechanical and optical

#96331 - $15.00 USD Received 16 May 2008; revised 17 Jul 2008; accepted 17 Jul 2008; published 24 Jul 2008
(C) 2008 OSA

characterization of this paper of one of these: the double-convex lens depicted in Fig. 1(c). This lens combined a plano-convex poly (methyl methacrylate) (PMMA) lens, R=25.8 mm, with a tunable elastomeric lens membrane, R=38.6 mm. The PMMA is rigid; the variable focal length is provided by elastomer side only. The PMMA and tunable lens membrane were designed to have diameters of 15 mm. The styrene-ethylene/butylene-styrene (SEBS) lens spacer was 4 mm thick with an inner and outer diameter of 20 and 25 mm respectively. After assembly, the double-convex lens design had an overall thickness of 8 mm.

2.2 Actuation

The lenses were designed to vary focal length based on a change in the deformable membrane shape with applied pressure, Fig. 2. Pressure to deform the lens is applied through surface contact with rigid rings. Squeezing the rings together displaces the soft, deformable cross-linked PDMS lens center. The pressure is converted into expansion of the SEBS membrane, resulting in a shape change of the outer surface. As the surface expands its average radius of curvature is reduced.

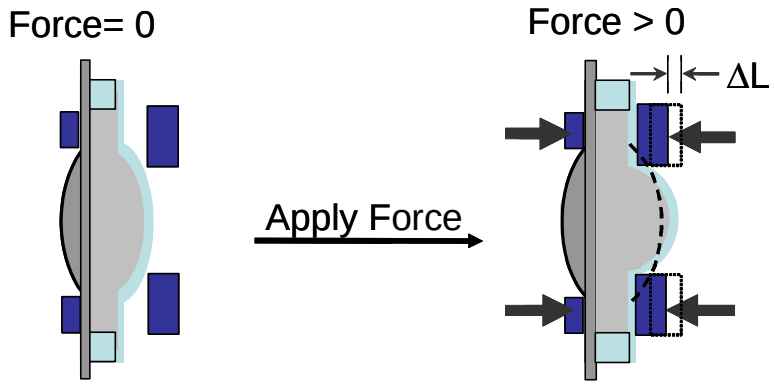

Fig. 2. Schematic of the mechanism for variable focal length. Pushing a plunger a distance ΔL causes the deformable elastomer within the lens to expand out against the pliable outer membrane. Dashed lines indicate plunger and surface locations before compression. Little compression is necessary; the maximum ΔL cited here is 1.28 mm.

Experimental induction of the SEBS membrane shape change was achieved using lens mounts. The mounts were designed with the membrane side of the lens held fixed against a circular aperture. A threaded retaining ring secured the lens from the back side, against the hard PMMA backing. Once engaged, the retaining ring could be further rotated inducing a uniform compressive force on the soft lens, which would drive the shape change of the deformable membrane.

The front aperture dimensions of the lens mount for all lens surface measurements was 3 mm thick with a diameter of 10.5 mm. The thread for the retaining ring required 1.56 turns to compress the lens by 1 mm. A typical linear force required for maximum reversible lens compression was 10 N.

Full optical simulations of the lenses have been performed, but their basic operation can be illustrated by simplified equations. Considering the biconvex lens to be comprised of two lenses, a PMMA lens and a tunable lens, the focal length of the system $F_{Composite}$ can be approximated by Eq. (1)

$$\frac{1}{F_{Composite}} \approx \frac{1}{F_{PMMA}} + \frac{1}{F_{Tunable}} \tag{1}$$

#96331 - $15.00 USD Received 16 May 2008; revised 17 Jul 2008; accepted 17 Jul 2008; published 24 Jul 2008
(C) 2008 OSA

The focal length of the tunable lens is proportional to its radius of curvature R. If an uncompressed lens with a radius of curvature R_o results in a tunable-part focal length of F_o, then the system focal length can be approximated by Eq. (2):

$$\frac{1}{F_{Composite}} \approx \frac{1}{F_{PMMA}} + \frac{R_o}{F_o R} \tag{2}$$

The shape change is reversible so long as the applied strain is within the elastic limit. The limit in tunable lens curvature occurs when the plunger is fully depressed. The minimum radius of curvature is practically limited to half the diameter of the optical aperture.

2.3 Surface profiles

Lens surface profiles were measured directly using a non-contact, raster-scanned depth measurement device. Three-dimensional maps of lens surfaces were measured by raster-scanning a range finder (Model Acuity AR200, Schmitt Measurement Systems, Inc. Portland, Oregon) across the face of the lens. The range finder operated by triangulating the position of a laser beam scattered off the surface. The device could measure distances up to 6.35 mm with a root-mean-squared measurement error of 5.8 μm, determined by running the profiler over a flat laser mirror set at a slight (3.4 deg) angle from normal incidence. The translation stage actuators had specified linear positioning repeatability better than 1 μm. Points across the surface were acquired on a 150 μm grid.

A consequence of the measurement geometry is that areas of the lens surface near the mount aperture were inaccessible to proper depth measurements. Two effects contributed to this loss of data: 1) obstruction of the profiler laser spot by the lens mount, and 2) multiple reflections of the laser between the lens surface and surrounding mount. Both of these effects can be traced to the fact that the lens is recessed from the mount surface: when viewed from an oblique angle (required for triangulation) the aperture side walls permitted a view only of an elliptical portion of the lens, and near the edges the profiler laser beam would reflect onto the walls and produce multiple spots.

To discriminate against edge effects, data near the edge were masked out. To discriminate against outliers, a spherical fit was performed to the remaining data and points deviating from the fit by more than a certain threshold were ignored. The threshold was typically 200 μm, 35x greater than the measurement uncertainty, and not less than 100 μm.

To test the accuracy of the measurement, an Edmund Optics NT45-084 glass lens was scanned. The manufacturer reports the 12 mm diameter lens has a surface with a 9.42 mm ± 1% radius of curvature. When scanned and fitted, the data showed a value of 9.54 mm radius of curvature with a standard deviation of 8.2 μm for the residuals.

Measurements were obtained for a variety of compression values, spanning a broad range of curvatures. The resulting datasets were compared against models for the surface shape, with the goals of predicting optical performance and providing physical insight into the membrane dynamics. The overall results of the data fitting are presented in Table 2, with an explanation of the parameters to follow.

First, the surface curvature scans were fit to a spherical profile. A spherical surface is described by an equation with one constant c:

$$z = \frac{c\left(x^2 + y^2\right)}{1 + \sqrt{1 - c^2\left(x^2 + y^2\right)}} \tag{3}$$

where the vertex of the spherical surface is located at (x, y, z) = (0, 0, 0), the radius of curvature is $R = 1/c$, and the surface curves upward into the space $z > 0$. In order to fit this curve to experimentally-determined data points, three additional parameters (x_o, y_o, z_o) are

#96331 - $15.00 USD Received 16 May 2008; revised 17 Jul 2008; accepted 17 Jul 2008; published 24 Jul 2008
(C) 2008 OSA

necessary to represent the location of the vertex, for a total of 4 fit coefficients. The results of the spherical fits are presented in Table 2. The radius of curvature shows a clear, monotonic decrease with increasing compression, ΔL. The membrane deforms to accommodate the pressure induced on the partially cross-linked polymer reservoir. The measured radius of curvature was reduced by nearly a factor of 4 for a total compression of only 1.12 mm.

Table 2: The first two sections present results of surface fits to measured surfaces as a function of plunger displacement ΔL. The standard deviation of the difference between data points and the fit is given in microns, and all other parameters are outlined in the text. The last section presents focal length information, both predicted and observed back focal lengths, and the resulting overall focal lengths. Uncertainty in the observed focal lengths is 0.5mm.

Spherical Fits				Biconic Fits					Back Focal Lengths			
ΔL (mm)	c(mm^{-1})	R (mm)	Stdev (μm)	c_x(mm^{-1})	c_y(mm^{-1})	k_x	k_y	Stdev (μm)	ΔL (mm)	Pred. (mm)	Obs. (mm)	F.L. (mm)
0.00	0.0366	27.32	10.71	0.0402	0.0336	-10.00	6.14	9.32	0	24.6	24.9	29.8
0.16	0.0397	25.19	12.95	0.0452	0.0354	-8.00	4.80	9.28	0.32	23.3	24.1	28.1
0.32	0.0507	19.72	9.16	0.0553	0.0556	-8.59	-7.44	8.49	0.64	18.9	17.6	22.8
0.48	0.0737	13.57	9.51	0.0829	0.0814	-5.40	-3.63	7.86	0.96	14.8	14.6	18.0
0.64	0.0943	10.60	8.85	0.1006	0.1027	-1.80	-2.24	7.29	1.28	12.9	13.0	15.8
0.80	0.1060	9.43	7.57	0.1147	0.1173	-1.18	-1.44	6.75				
1.12	0.1381	7.24	13.05	0.1321	0.1344	0.50	0.35	11.69				

Initially, the lens assumes a more spherical shape with compression. At compression values of ΔL = 0.32 to 0.80 mm, the standard deviations are near the instrument limit of 8.2 μm, as determined by measuring a commercial-quality control lens. At the highest compressions the deviation from a sphere increases rapidly. Much of this residual deviation is near the lens edges, suggesting a systematic departure from a spherical surface at large compression. This is not surprising given the lens mount geometry and reduced curvature. The plunger aperture is 10.5 mm in diameter; as the radius of curvature approaches half this (5.25 mm) the edges can be expected to deviate from spherical.

The spherical fits of Table 2 provided a first order measure of the focal length of the variable lens. More sophisticated models for the shape of the surface were applied in order to track the optical aberrations and to give a better understanding of how the membrane deforms. To extend the surface model beyond a simple sphere, one choice is to employ a polynomial expansion such as Zernike polynomials, which are commonly used in the analysis of optical aberrations. Instead extension of the data analysis with a biconic surface was performed which should provide more physical insight into the membrane shape. The biconic surface is described by

$$z = \frac{c_x\ x^2 + c_y\ y^2}{1 + \sqrt{1 - \left(1 + k_x\right)\ c_x{}^2 x^2 - \left(1 + k_y\right)\ c_y{}^2 y^2}} \qquad (4)$$

which deviates from a sphere via a conic constant k and furthermore allows for astigmatism through separate values for the curvature $(c_x, c_y) = (1/R_x, 1/R_y)$ and conic constant (k_x, k_y) along each axis $\boldsymbol{x}$ & $\boldsymbol{y}$. The advantages of this description include the fact that it requires relatively few parameters to describe the surface (four) and that a clear, physical meaning can be ascribed to each one. In particular, physical intuition suggests that the surface shape will be stretched almost linearly near the lens aperture. This would suggest a cross section more hyperbolic than circular, which is precisely what the conic constant k allows one to model. Along either axis, the physical meaning of the conic constant k can be described loosely by saying at values of $k > 0$ the surface curves away more sharply than for a sphere, while for

#96331 - $15.00 USD Received 16 May 2008; revised 17 Jul 2008; accepted 17 Jul 2008; published 24 Jul 2008
(C) 2008 OSA

values of $k < 0$ the surface curves away more shallowly than for a sphere. More precisely, the curve is a hyperbola for values of $k < -1$, a parabola for $k = -1$, an ellipse for $-1 < k < 0$, a circle for $k = 0$, and an oblate ellipsoid for $k > 0$. It should be pointed out that fitting these data requires several more degrees of freedom than the four mentioned here. The experimental axes (x,y,z) in the lab frame were related to the principal (X,Y,Z) axes of a biconic lens through the incorporation of additional translational (3) and rotational (3) degrees of freedom in the actual surface fit.

The results of biconic surface curvature fits are shown in Table 2. As anticipated the conic constants for most of the fits are negative, suggestive of hyperbolic shapes where the center of the membrane is spherical while the edges trail off nearly linearly towards the inner boundary of the plunger. As the compression increases, however, there is a shift towards higher conic constants until, at the highest compression, the constant flips sign. We speculate that at this high compression the center of the membrane is reaching a saturation point in its expansion, causing it to flatten out some and make the edges look steeper by comparison. An important point is that ahead of that transition region the lens surface is very well described by a sphere, which should translate to good optical performance.

To gain a deeper understanding of the deformation behavior of the dynamic surface, one would have to consider the strain distribution on the surface that is likely balanced biaxial at the center and gradually becomes uniaxial at the edges. Furthermore, one would expect the magnitude of the strain to be greater at the center [20]. This strain distribution, the stress-strain behavior of the material in both biaxial and uniaxial loading, and the boundary conditions imposed by the rigid rings during deformation would all contribute to the deformation behavior. A deformation analysis considering these parameters is possible, especially with the aid of finite element methods, but is beyond the purpose and scope of this paper.

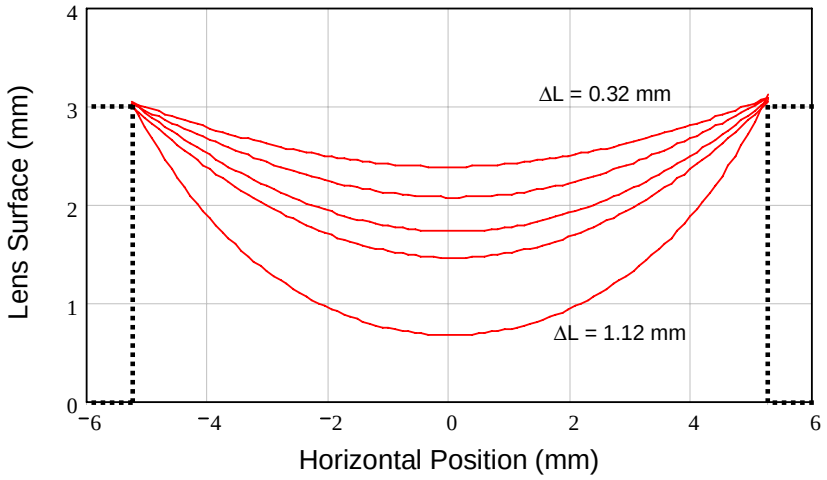

Fig. 3. Plot of surface profiles as interpolated from fitted measurements. Dotted lines represent lens mount.

Conic constants describe the deviation of a surface from a sphere. The biconic fit also enables us to describe the asymmetry, or astigmatism, of a lens. We can investigate the degree of astigmatism by computing the difference in height along orthogonal directions across the lens surface. The data show that the lens surface goes through a minimum astigmatism near $\Delta L = 0.64$ mm, at which point the maximum deviation of one curve from the other is 10 μm out at the lens edge. Since the averaged sag at this point is 1.3 mm, this represents a relative astigmatism < 1%. The largest astigmatism is measured for a low-

#96331 - $15.00 USD Received 16 May 2008; revised 17 Jul 2008; accepted 17 Jul 2008; published 24 Jul 2008
(C) 2008 OSA

pressure case ΔL = 0.16 mm. Here is measured a maximum deviation from symmetry of 57 μm out of a total sag of 0.52 mm, for a relative astigmatism of 11%.

Shown in Fig. 3 are cross-sections of the lens profile under different amounts of strain. The data presented are generated from spherical curve fits and are graphed in a coordinate system in which the outer face of the lens mount lies along y=0. The data points within a single curve are accurate with respect to one another, but different curves may be offset horizontally by up to 0.3 mm as a result of the uncertainty in accurately registering the edge of the aperture mount.

As the strain/pressure is increased the lens surface wells up to form a boundary with greater and greater curvature. The maximum displacement of the central surface is about 2 mm. Not shown are the curves for ΔL = 0 and 0.16 mm. Below ΔL = 0.32 mm, the mount did not fully engage the lens surface. The surface was in contact only on one side of the aperture, which helps to explain the higher standard deviations of the low-compression surface fits in Table 1.

Future work correlating the volume redistribution of the tunable lens as a function of elastic membrane response and plunger position may be considered to better predict optical behaviors of these novel, solid state tunable lenses.

2.4 Optical properties

To test the optical performance of the lens, images of simple objects were projected onto a CCD camera. To measure back focal lengths, a 2.5 cm tall printed "Y" was placed 1 meter away from a camera. The lens was mounted on a translation stage in front of a camera. The back focal length was measured by recording the stage position at which the image was in focus, measuring the distance between the camera plane and the lens mount, and accounting for the surface deformations induced by the lens compression. The software used to model the optical properties of the lens was ZEMAX, written by the ZEMAX Development Corporation, Bellevue, WA. Inputs into the model were spherical fit results from measurements of both sides of the lens, including the pressure-induced center thickness changes mentioned above.

Object and image distances were compared to optical calculations carried out in a standard optical design software package. The results of the spherical surface fits in Table 1, the geometry of the various lens components from Fig. 1, and the refractive indices as reported in Table 2 were used as inputs to the software. Measurements were carried out at several lens compression values to see how the lens performed at different focal lengths. Table 1 shows a comparison of fitted and measured back focal lengths. The agreement is excellent, suggesting that the principal properties of these lenses can be well-understood from a detailed knowledge of their composition and shape change. Based on this good agreement, the calculated effective focal length is reported as a function of the compression ΔL. The focal length, and therefore the optical power, of the lens varied by nearly a factor of two with a ΔL of only 1.28 mm. This is directly verified by comparing the image sizes recorded for each compression value: for a distant object the magnification is proportional to the focal length.

A metric for the optical power in a lens is the diopter, defined as 1/focal length in inverse meters. This metric is most useful when comparing lenses of a similar aperture. Because of the inverse relationship, small changes to small focal lengths can correspond to large diopter changes, but systems with small lenses necessarily operate in a different regime than systems with larger lenses. For our lens with its 10.5 mm aperture, we observe a tunable variation of 30 diopters, which represents a significant change in optical power. For example, the human eye can effect a change of only ~4 diopters [1]. The change in optical power of the lens described here is similar to that reported in the referenced literature for tunable lenses with a comparable diameter. Of the reported lenses with apertures of 5 mm or greater, only three have a greater change in optical power. Two 5 mm aperture lenses [11, 13] were reported to

#96331 - $15.00 USD Received 16 May 2008; revised 17 Jul 2008; accepted 17 Jul 2008; published 24 Jul 2008
(C) 2008 OSA

exhibit tunable changes of 52 and 45 diopters respectively. A change in power of 150 diopters was reported for a 20 mm diameter lens [7] but this was achieved by adjusting two optical surfaces simultaneously.

Fig. 4. Images acquired at two different zoom states of the lens. The magnification of the object in these images differs by a factor of 1.8.

Quantitative assessments of the image quality of the lenses, such as measurements of the modulation transfer function, are beyond the scope of this introductory paper. Sample images are presented in Fig. 4. Qualitatively, the image quality tracked the behavior observed in the surface profile fits: trailing off at the extremes of compression but quite good over a large range in the middle. Images in all cases were easily recognizable and, by eye, free of distortion. At the lower end of the compression range the quality is expected to improve with a more symmetric initial lens construction. (Preliminary efforts along this direction have already shown improvement at low compression.) At the upper end of the range the quality is limited not by issues of lens construction but rather by the inherent aberrations of highly-curved optical surfaces. Nonetheless, there are at least two ways in which the upper end of the range could be addressed, both related to the many degrees of freedom afforded by the construction of these lenses. They are: 1) the use of higher-index materials in the lens, and 2) utilizing the conic constants of the surface membrane to correct for aberrations. Higher-index materials would allow for greater focal length changes with less curvature. This automatically entails less aberration for the same power change: less curvature results in less aberration. The conic constants can also help. For highly-curved surfaces, a negative conic constant helps reduce spherical aberration. By tailoring the mechanical properties of the membrane one could achieve a membrane that could adopt target deformation characteristics as a function of compression – improving optical quality as a result.

3. Conclusion

In conclusion, we have demonstrated a general technique for making variable focal length lenses. Their construction is easily generalized to compound lenses which can have negative focal lengths, positive focal lengths, or lenses that can switch between positive and negative, which is required for high zoom ratios with stationary lenses. Based on the compression of a reservoir or sac of gel-like polymer, the convex lens surface is formed by an elastic membrane that expands outward in response to the applied pressure. Experimental surface profiles of the elastomeric membrane were fitted to spherical and biconic shapes to predict lens focal length and image properties as a function of compression. As a result of the surface profile measurements, predictions of the optical behavior were in very good agreement with the observed data. By compressing the reservoir only 1.3 mm we changed the focal length of the lens by a factor of 1.9. Dynamically-magnified images generated by the lens show the usefulness of these lenses as working optical elements and have led to preliminary demonstrations of unique camera designs.

#96331 - $15.00 USD Received 16 May 2008; revised 17 Jul 2008; accepted 17 Jul 2008; published 24 Jul 2008
(C) 2008 OSA

Acknowledgments

The authors would like to acknowledge funding received from DARPA, and valuable discussions with L. Buckley, D. Scribner, R. Stroman, E. Fleet, H. Ricks-Laskoski, and A. Snow.

#96331 - $15.00 USD Received 16 May 2008; revised 17 Jul 2008; accepted 17 Jul 2008; published 24 Jul 2008
(C) 2008 OSA